Inorg. Chem. **2005**, *44*, 1686–1692

Silver(I) Compounds Consisting of [2.2]Paracyclophane: Reversible Guest-Driven Solid-State Transformation and Incorporation Behavior

Takayoshi Kuroda-Sowa, Shu Qin Liu, Yuji Yamazaki, Megumu Munakata,* Masahiko Maekawa, Yusaku Suenaga, Hisashi Konaka, and Hisao Nakagawa

Department of Science, Kinki University, Higashi-Osaka, Osaka 577-8502, Japan

Received May 24, 2004

Reaction of [2.2]paracyclophane with silver(I) heptafluorobutyrate ($AgC_3F_7CO_2$) has isolated three novel networks: $[Ag_4(pcp)(C_3F_7CO_2)_4]$·pyrene (**1**), $[Ag_4(pcp)(C_3F_7CO_2)_4]$·phen (phen = phenanthrene) (**2**), and $[Ag_4(pcp)(C_3F_7CO_2)_4]$·fluorene (**3**), and an intercalation compound $[Ag_4(pcp)(C_3F_7CO_2)_4]$·2benzene (**4**). All the four complexes exhibit two-dimensional (2D) sheet structures in which $AgC_3F_7CO_2$ form an infinite chain and pcp acts as linkage. **1**, **2**, and **3** show 2D flat sheets with cavities in which guest molecules are situated, whereas **4** exhibits 2D zigzag layers between which guest benzene molecules are intercalated. Pcp shows μ-di-η^1-η^2 coordination mode in **1**, μ-tetra-η^1 coordination mode in **2** and **3**, and μ-tetra-η^2 coordination mode in **4**. The reversible guest exchanges were observed between complex **1**, **2**, or **3** and intercalation compound **4**. It is unprecedented for metal–organic inclusion complexes that the guest exchange occurs where the guest is the solute molecule. Furthermore, **4** can release the guest, and the original framework was completely recovered after reincorporation of benzene. It should be noted that **4** can incorporate pyrene, phen, and fluorene to give **1**, **2**, and **3**, respectively, after desorption.

1. Introduction

Metal−organic frameworks containing cavities or channels have attracted current interest because of their functional properties,[1−6] which are similar to those found in zeolites and clays. Recent effort has been devoted to the development of porous materials that show crystal-to-crystal transformation caused by anion exchange[7] or guest exchange.[8] However, reports on reversible structural transformation triggered by guest exchange are very sparse.[8b] Furthermore, almost all previous work on the development of porous metal−organic framework has featured N- or O-donor bridging ligands.[1−8] In this paper, we select [2.2]paracyclophane (pcp) to construct networks with cavities. The most important feature of pcp, compared with those mentioned above, is that it does not contain heteroatoms. Consequently, the coordination

* To whom correspondence should be addressed. Email: munakata@chem.kindai.ac.jp. Telephone: +81-6-6730-5880 ext. 4001 or 4119. Fax: +81-6-6723-2721. Department of Science, Kinki University, Kowakae 3-4-1, Higashi-Osaka, Osaka 577-8502, Japan.

(1) (a) Chen, B.; Eddaoudi, M.; Hyde, S. T.; O'Keffe, M.; Yaghi, O. M. *Science* **2001**, *291*, 1021. (b) Lu, J.; Mondal, A.; Moulton, B.; Zaworotko, M. J. *Angew. Chem., Int. Ed.* **2001**, *40*, 2113. (c) Noro, S.-I.; Kitagawa, S.; Kondo, M.; Seki, K. *Angew. Chem., Int. Ed*. **2000**, *39*, 2081. (d) Seo, J.-S.; Whang, D.; Lee, H.; Jun, S. I.; Oh, J.; Jeon, Y. J.; Kim, K. *Nature* **2000**, *404*, 982. (e) Chui, S. S.-Y.; Lo, S. M.-F.; Charmant, J. P. H.; Orphen, A. G.; Williams, I. D. *Science* **1999**, *283*, 1148. (f) Goodgame, D. M. L.; Grachvogel, D. A.; Williams, D. J. *Angew. Chem., Int. Ed*. **1999**, *38*, 153.

(2) (a) Batten, S. R.; Robson, R. *Angew. Chem., Int. Ed*. **1998**, *37*, 1460. (b) Zaworotko, M. J. *Chem. Commun*. **2001**, 1. (c) Yaghi, O. M.; Li, H.; Davis, C.; Richardson, D.; Groy, T. L. *Acc. Chem. Res*. **1998**, *31*, 474. (d) Kitagawa, S.; Kondo, M. *Bull. Chem. Soc. Jpn*. **1998**, *71*, 1739. (e) Fujita, M.; Kwon, Y. J.; Washizu, S.; Ogura, K. *J. Am. Chem. Soc*. **1994**, *116*, 1151.

(3) (a) Li, H.; Eddaoudi, M.; Groy, T. L.; Yaghi, O. M. *J. Am. Chem. Soc*. **1998**, *120*, 8571. (b) Reddy, D. S.; Duncan, S.; Shimizu, G. K. H. *Angew. Chem., Int. Ed*. **2003**, *42*, 1360. (c) Kitaura, R.; Fujimoto, K.; Noro, S.-I.; Kondo, M.; Kitagawa, S. *Angew. Chem., Int. Ed*. **2002**, *41*, 133.

(4) (a) Biradha, K.; Hongo, Y.; Fujita, M. *Angew. Chem., Int. Ed*. **2000**, *39*, 3843. (b) Lu, J. Y.; Babb, A. M. *Chem. Commun*. **2003**, 1346.

(5) (a) Farrell, R. P.; Hambley, T. W.; Lay, P. A. *Inorg. Chem*. **1995**, *34*, 757. (b) Papaefstathiou, G. S.; MacGillivray, L. R. *Angew. Chem., Int. Ed*. **2002**, *41*, 2070. (c) Kepert, C. J.; Prior, T. J.; Rosseinsky, M. J. *J. Am. Chem. Soc*. **2000**, *122*, 5158.

(6) (a) Tabares, L. C.; Navarro, J. A. R.; Salas, J. M. *J. Am. Chem. Soc*. **2001**, *123*, 383. (b) Soldatov, D. V.; Ripmeester, J. A.; Shergina, S. I.; Sokolov, I. E.; Zanina, A. S.; Gromilov, S. A.; Dyadin, Y. A. *J. Am. Chem. Soc*. **1999**, *121*, 4179. (c) Alberti, G.; Murcia-Mascaros, S.; Vivani, R. *J. Am. Chem. Soc*. **1998**, *120*, 9291.

(7) (a) Min, K. S.; Suh, M. P. *J. Am. Chem. Soc*. **2000**, *122*, 6834. (b) Jung, O.-S.; Kim, Y. J.; Lee, Y.-A.; Park, J. K.; Chae, H. K. *J. Am. Chem. Soc*. **2000**, *122*, 9921. (c) Jung, O.-S.; Kim, Y. J.; Lee, Y.-A.; Park, J. K.; Chae, H. K.; Hong, J. *Inorg. Chem*. **2001**, *40*, 2105. (d) Noro, S.-I.; Kitaura, R.; Kondo, M.; Kitagawa, S.; Ishii, T.; Matsuzaka, H.; Yamashita, M. *J. Am. Chem. Soc*. **2002**, *124*, 2568.

(8) (a) Biradha, K.; Hongo, Y.; Fujita, M. *Angew. Chem., Int. Ed*. **2002**, *41*, 3395. (b) Kurmoo, M.; Kumagai, H.; Hughes, S. M.; Kepert, C. J. *Inorg. Chem*. **2003**, *42*, 6709. (c) Suh, M. P.; Ko, J. W.; Chio, H. J. *J. Am. Chem. Soc*. **2002**, *124*, 10976. (d) Zeng, M. H.; Feng, X. L.; Chen, X. M. *J. Chem. Soc., Dalton Trans*. **2004**, 2217.

10.1021/ic0400742 CCC: $30.25
Published on Web 02/18/2005

polymers of pcp with silver(I) are not constructed by metal−heteroatom bonds, but by metal−π bonds. Although previous work has already demonstrated the possibility of using metal−π bonds to direct the assembly of networks,[9] reports are still lacking on networks with cavities that are constructed by metal−π bonds and show reversibly structural transformation triggered by guest exchange. Herein, we present three novel complexes $[Ag_4(pcp)(C_3F_7CO_2)_4]$·pyrene (**1**), $[Ag_4(pcp)(C_3F_7CO_2)_4]$·phen (**2**) (phen = phenanthrene), and $[Ag_4(pcp)(C_3F_7CO_2)_4]$·fluorene (**3**) and an intercalation compound $[Ag_4(pcp)(C_3F_7CO_2)_4]$·2benzene (**4**) that are constructed by pcp and silver(I) through metal−π bonds. **1**, **2**, and **3** can exchange the guest molecules (pyrene, phen, and fluorene, respectively) for benzene to afford **4** and vice versa. **4** exhibits reversible incorporation of guest benzene. Additionally **4** can incorporate pyrene, phen, and fluorene to give **1**, **2**, and **3**, respectively, after desorption.

2. Experimental Section

2.1. General Procedures. All reactions and manipulations were carried out under an argon atmosphere by using the usual Schlenk techniques. Solvents were dried and distilled by standard methods prior to use and stored under argon. Reagent grade $AgC_3F_7CO_2$ and pcp were purchased from Aldrich. All chemicals were used as received without further purification. IR spectra were recorded with KBr disks on a JASCO FT/IR 8000 spectrometer. ^{1}H NMR spectra were measured on a JEOL GSX 270 FT NMR spectrometer at room temperature. Tetramethylsilane was used as an internal reference for ^{1}H NMR measurement. TG analyses were performed at 10 °C min^{-1} under nitrogen on Rigaku Thermo plus TG 8120. X-ray powder diffraction (XRPD) data were recorded on a Rigaku Rint 2000 diffractometer at 40 kV, 80 mA for Cu Kα (λ = 1.54056 Å), with a scan speed of 8 deg/min and step size of 0.06° in 2θ at room temperature.

2.2. Syntheses. $[Ag_4(pcp)(C_3F_7CO_2)_4]$·Pyrene (1). This complex was prepared by mixing $AgC_3F_7CO_2$ (128.2 mg, 0.4 mmol) and pcp (20.8 mg, 0.1 mmol) in 10 mL of mesitylene. After stirring for 30 min, pyrene (303.9 mg, 1.5 mmol) was added to the resulting solution for reaction for 30 min. The colorless block crystals of **1** were obtained by layering tetradecane onto the above solution for 1 week at room temperature. Yield: 112.5 mg (6.64×10^{-2} mmol, 66.4%). Anal. Calcd for $Ag_4F_{28}O_8C_{48}H_{26}$: C 34.03, H 1.55. Found: C 34.17, H 1.59. ^{1}H NMR (acetone-d_6): δ H 3.09 (CH_2, pcp), 6.54 (phenyl, pcp), 8.04−8.30 (CH, pyrene). IR (KBr, ν/cm^{-1}): 3046(w), 2951(w), 2926(w), 2887(w), 2851(w), 1681(s), 1503(w), 1411(m), 1340(m), 1275(m), 1220(s), 1157(s), 1117(m), 1083(m), 967(m), 936(m), 893(w), 852(m), 840(m), 743(m), 719(m), 623(w), 586(w), 528(w), 509(w).

$[Ag_4(pcp)(C_3F_7CO_2)_4]$·Phen (2). The colorless plate crystals of **2** were grown similarly to those of **1** using phenanthrene (276.4 mg, 1.5 mmol) instead of pyrene. Yield: 103.1 mg (6.17×10^{-2} mmol, 61.7%). Anal. Calcd for $Ag_4F_{28}O_8C_{46}H_{26}$: C 33.08, H 1.57. Found: C 34.17, H 1.59. ^{1}H NMR (acetone-d_6): δ H 3.09 (CH_2, pcp), 6.54 (phenyl, pcp), 8.04−8.07, 8.09, 8.18−8.30 (CH, phen). IR (KBr, ν/cm^{-1}): 3046 (w), 2950 (w), 2926 (w), 2887 (w), 2850 (w), 1681 (s), 1503 (w), 1411 (m), 1340 (m), 1275 (m), 1220 (s), 1157 (s), 1117 (m), 1083 (m), 967 (m), 936 (m), 893 (w), 852 (m), 840 (m), 743 (m), 719 (m), 625 (w), 586 (w), 527 (w), 509 (w).

$[Ag_4(pcp)(C_3F_7CO_2)_4]$·Fluorene (3). The colorless block crystals of **3** were obtained similarly to those of **1** using fluorene (900 mg, 6.0 mmol) instead of pyrene. Yield: 100.8 mg (6.08×10^{-2} mmol, 60.8%). Anal. Calcd for $Ag_4F_{28}O_8C_{45}H_{26}$: C 32.60, H 1.58. Found: C 32.33, H 1.58. ^{1}H NMR (acetone-d_6): δ H 3.08 (CH_2, pcp), 6.55 (phenyl, pcp), 3.92 (CH_2, fluorene), 7.27−7.41, 7.56−7.60, 7.85−7.88 (CH, fluorene). IR (KBr, ν/cm^{-1}): 3045 (w), 2946 (w), 2926 (w), 2850 (w), 1684 (s), 1638 (s), 1488 (w), 1451 (m), 1411 (m), 1338 (m), 1215 (s), 1121 (s), 1085 (m), 967 (m), 934 (m), 895 (m), 817 (m), 755 (m), 717 (m), 634 (w), 596 (w), 528 (w), 507 (w).

$[Ag_4(pcp)(C_3F_7CO_2)_4]$·2Benzene (4). The colorless plate crystals of **4** were grown similarly to those of **1** using benzene instead of mesitylene in the absence of pyrene. Yield: 37.4 mg (2.27×10^{-2} mmol, 22.7%). Anal. Calcd for $Ag_2F_{14}O_4C_{22}H_{14}$: C 32.07, H 1.71. Found: C 32.56, H 1.76.^{1}H NMR (acetone-d_6): δ H 3.08 (CH_2, pcp), 6.54 (phenyl, pcp), 7.35 (phenyl, benzene). IR (KBr, ν/cm^{-1}): 3033 (w), 3013 (w), 2952 (w), 2927 (w), 2888 (w), 2852 (w), 1683 (s), 1500 (w), 1411 (m), 1340 (m), 1275 (m), 1222 (s), 1189 (s), 1158 (m), 1117 (m), 1083 (m), 968 (m), 935 (m), 895 (w), 815 (m), 766 (w), 743 (m), 719 (m), 623 (w), 586 (w), 527 (w), 509 (w).

2.3. X-ray Data Collection and Structure Solutions and Refinements. A suitable single crystal was fixed on a glass fiber, and diffraction data were collected at −123 °C on a Rigaku/MSC Mercury CCD diffractometer with graphite-monochromated Mo Kα radiation (λ = 0.71070 Å) by the ω scan mode. A symmetry-related absorption correction was applied that resulted in transmission factors ranging from 0.72 to 0.85 for **1**, 0.72 to 0.97 for **2**, 0.70 to 0.77 for **3**, and 0.67 to 0.84 for **4**. All intensity data were corrected for Lorentz and polarization effects.

The structures were solved by direct methods,[10] expanded using Fourier techniques,[11] and refined by full-matrix least-squares analysis on F^2 using the TEXSAN package.[12] All the full-occupancy non-hydrogen atoms were refined anisotropically. Hydrogen atoms of all the structures were introduced in their calculated positions. They were included but not refined in the refinement. Details of X-ray experiments and crystal data are summarized in Table 1. Selected bond lengths and bond angles are given in Table 2.

3. Results and Discussion

3.1. Description of the Structures. $[Ag_4(pcp)(C_3F_7CO_2)_4]$·Pyrene (1). The crystal structure of **1** revealed that the two crystallographically independent silver(I) ions are bridged by two carboxylate groups to form an eight-membered ring $Ag_2O_2C_4$ (Figure 1a), and these rings are linked by Ag−O bonds via rhombic ring Ag_2O_2 to give a ribbonlike chain consisting of $AgC_3F_7CO_2$ as shown in Figure 1b. The tetrahedral Ag(1) is bonded to three O atoms from three different $C_3F_7CO_2^-$ groups and one C atom of pcp, while Ag(2) is bridged by three O atoms from three distinct $C_3F_7CO_2^-$ groups and one C=C moiety of pcp. The Ag−O and Ag−C bond lengths are comparable with those of silver(I)−polycyclic aromatic hydrocarbon.[13] Each pcp exhibits a μ-di-η^1-η^2 coordination mode symmetrically bridging four metal centers with two on the upper and lower decks

(9) Munakata, M.; Wu, L. P.; Ning, G. L. *Coord. Chem. Rev.* **2000**, *198*, 171 and references therein.

(10) Gilmore, C. J. *J. Appl. Crystallogr.* **1984**, *17*, 42.

(11) Beurskens, P. T. *DIRDIF94: Direct Methods for Different Structures: An Automatic Procedure for Phase Extension and Refinement of Different Structure Factors, Technical Report*; Crystallographic Laboratory: University of Nijimegen, The Netherlands, 1994; Vol.1.

(12) *TEXSAN-TEXRAY: Structure Analysis Package*; Molecular Structure Corp.: The Woodlands, TX, 1985 and 1999.

Table 1. Crystallographic Data for Complexes **1**−**4**

	1	**2**	**3**	**4**
formula	$C_{48}H_{26}Ag_4F_{28}O_8$	$C_{46}H_{26}Ag_4F_{28}O_8$	$C_{45}H_{26}Ag_4F_{28}O_8$	$C_{44}H_{28}Ag_4F_{28}O_8$
formula weight	1694.16	1670.13	1658.12	1648.13
crystal system	triclinic	triclinic	triclinic	triclinic
space group	$P\bar{1}$(No. 2)	$P\bar{1}$(No. 2)	$P\bar{1}$(No. 2)	$P\bar{1}$(No. 2)
a, Å	10.8793(2)	10.902(5)	10.863(2)	9.89(2)
b, Å	11.7609(6)	10.925(5)	10.971(2)	10.02(2)
c, Å	12.4095(3)	12.147(3)	12.106(2)	15.19(3)
α, deg	69.23(1)	100.18(3)	100.290(5)	105.59(2)
β, deg	80.88(2)	100.079(3)	99.477(2)	93.567(10)
γ, deg	58.91(1)	114.218(4)	114.622(6)	118.26(2)
V, Å^3	1270.8(2)	1248.4(9)	1243.6(4)	1245(3)
Z	1	1	1	1
ρ, g/cm^3	2.214	2.221	2.214	2.197
μ, cm^{-1}	16.72	17.00	17.06	17.03
measured reflections	5656	5450	5412	5424
observed reflections ($I > 2\sigma(I)$)	5250	4385	4489	4079
parameters	436	397	402	421
R^a ($I > 2\sigma(I)$)	0.032	0.033	0.031	0.043
$R_w{}^b$(all data)	0.078	0.069	0.072	0.090

^{a} $\sum||F_o| - |F_c||/\sum|F_o|$. ^{b} $[\sum w(F_o^2 - F_c^2)^2/\sum w(F_o^2)^2]^{1/2}$.

Table 2. Selected Bond Lengths (Å) and Angles (deg) for Complexes **1**−**4**

		Complex **1**			
Ag(1)−O(1)	2.278(2)	Ag(2)−O(2)″	2.442(3)	Ag(1)−O(4)′	2.447(2)
Ag(1)−C(6)	2.527(3)	Ag(2)−C(3)	2.691(3)	Ag(2)−O(3)	2.293(2)
Ag(2)−O(2)	2.337(2)	Ag(1)−O(4)	2.319(2)	Ag(2)−C(2)	2.461(4)
O(1)−Ag(1)−O(4)	129.91(9)	O(2)″−Ag(2)−C(3)	125.43(8)	O(2)−Ag(2)−C(2)	105.51(9)
O(4)−Ag(1)−O(4)′	74.89(8)	O(3)−Ag(2)−C(3)	94.82(9)	O(2)″−Ag(2)−C(2)	132.54(9)
O(4)−Ag(1)−C(6)	115.67(9)	O(1)−Ag(1)−O(4)′	105.45(7)	O(3)−Ag(2)−C(2)	120.6(1)
O(2)−Ag(2)−O(3)	122.33(6)	O(1)−Ag(1)−C(6)	108.84(9)	C(2)−Ag(2)−C(3)	31.15(9)
O(2)″−Ag(2)−O(3)	92.63(9)	O(4)′−Ag(1)−C(6)	116.0(1)		
O(2)−Ag(2)−C(3)	136.64(9)	O(2)−Ag(2)−O(2)”	78.15(8)		
		Complex **2**			
Ag(1)−O(1)	2.338(3)	Ag(2)−O(4)″	2.440(2)	Ag(2)−O(4)	2.328(2)
Ag(1)−O(3)	2.274(2)	Ag(1)−O(1)′	2.422(3)	Ag(2)−C(3)	2.455(4)
Ag(2)−O(2)	2.269(3)	Ag(1)−C(1)	2.478(4)		
O(1)−Ag(1)−O(1)′	76.01(10)	O(2)−Ag(2)−C(3)	113.53(9)	O(3)−Ag(1)−C(1)	118.3(1)
O(1)−Ag(1)−C(1)	113.26(9)	O(4)−Ag(2)−C(3)	110.92(10)	O(2)−Ag(2)−O(4)″	96.73(9)
O(1)′−Ag(1)−C(1)	108.1(1)	O(1)−Ag(1)−O(3)	123.70(9)	O(4)−Ag(2)−O(4)″	78.71(9)
O(2)−Ag(2)−O(4)	126.09(10)	O(1)′−Ag(1)−O(3)	106.72(9)	O(4)″−Ag(2)−C(3)	127.5(1)
		Complex **3**			
Ag(1)−O(1)	2.338(2)	Ag(2)−O(4)″	2.435(2)	Ag(2)−O(4)	2.328(2)
Ag(1)−O(3)	2.270(2)	Ag(1)−O(1)′	2.422(3)	Ag(2)−C(3)	2.458(4)
Ag(2)−O(2)	2.265(3)	Ag(1)−C(1)	2.495(3)		
O(1)−Ag(1)−O(1)′	76.30(9)	O(2)−Ag(2)−C(3)	113.67(9)	O(3)−Ag(1)−C(1)	117.1(1)
O(1)−Ag(1)−C(1)	112.71(9)	O(4)−Ag(2)−C(3)	110.97(9)	O(2)−Ag(2)−O(4)″	98.94(8)
O(1)′−Ag(1)−C(1)	105.6(1)	O(1)−Ag(1)−O(3)	124.91(9)	O(4)−Ag(2)−O(4)″	79.08(9)
O(2)−Ag(2)−O(4)	126.59(9)	O(1)′−Ag(1)−O(3)	108.88(9)	O(4)″−Ag(2)−C(3)	123.5(1)
		Complex **4**			
Ag(1)−O(1)	2.245(3)	Ag(2)−C(2)	2.373(5)	Ag(2)−O(4)″	2.420(6)
Ag(1)−O(3)′	2.418(6)	Ag(1)−O(3)	2.481(4)	Ag(2)−C(3)	2.619(4)
Ag(1)−C(6)	2.432(4)	Ag(1)−C(1)	2.422(6)		
Ag(2)−O(4)	2.432(3)	Ag(2)−O(2)	2.240(3)		
O(1)−Ag(1)−O(3)	89.8(1)	O(2)−Ag(2)−C(2)	136.8(2)	O(3)′−Ag(1)−C(1)	123.4(2)
O(1)−Ag(1)−C(1)	132.8(2)	O(4)−Ag(2)−O(4)″	85.9(1)	C(1)−Ag(1)−C(6)	33.2(2)
O(3)−Ag(1)−O(3)′	86.0(1)	O(4)″−Ag(2)−C(3)	92.1(2)	O(2)−Ag(2)−O(4)″	100.1(2)
O(3)−Ag(1)−C(6)	99.4(1)	O(1)−Ag(1)−O(3)′	92.5(1)	O(2)−Ag(2)−C(3)	167.1(2)
O(3)′−Ag(1)−C(6)	98.6(2)	O(1)−Ag(1)−C(6)	166.1(2)	O(4)−Ag(2)−C(3)	89.8(1)
O(2)−Ag(2)−O(4)	95.1(1)	O(3)−Ag(1)−C(1)	119.4(1)	C(2)−Ag(2)−C(3)	31.9(2)

of pcp, respectively. The pcp molecules link the ribbonlike $AgC_3F_7CO_2$ chains to form a weblike two dimensional (2D) flat sheet with cavities of 8.3 × 7.9 Å (Figure 1b), which are occupied by pyrene via edge-to-face $\pi-\pi$ interactions between host pcp and guest pyrene with the shortest H4···C24 distance of 2.70 Å.[14] The 2D layers are separated by 11.9 Å and packed in an offset mode as shown in Figure 2. No significant interactions are found between interlayers.

$[Ag_4(pcp)(C_3F_7CO_2)_4]\cdot$Phen (2). Similar to complex **1**, the crystal structure of **2** revealed that **2** contains a 2D network with cavities of 8.0 × 7.5 Å, in which the disordered phen molecules are situated via edge-to-face $\pi-\pi$ interac-

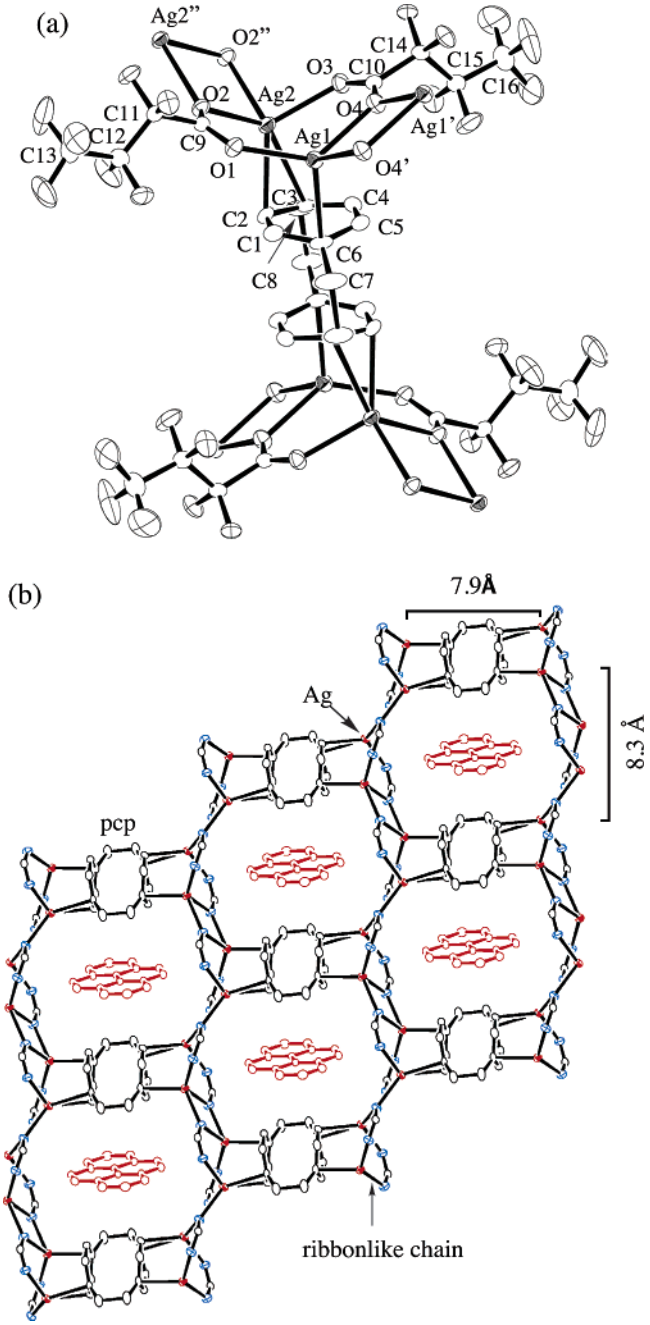

Figure 1. (a) Molecular structure and atom numbering scheme of **1**, showing the complete coordination of silver. (b) View down the *c*-axis of **1**, showing the 2D sheet with ordered pyrene molecules in cavities. All H atoms and C_3F_7 groups are omitted for clarity.

tions between host pcp and guest phen with the shortest H3···C23 distance of 2.70 Å. However, the coordination environment of silver(I) is different from that in **1**. Both the tetrahedral Ag(1) and Ag(2) are four coordinate, consisting

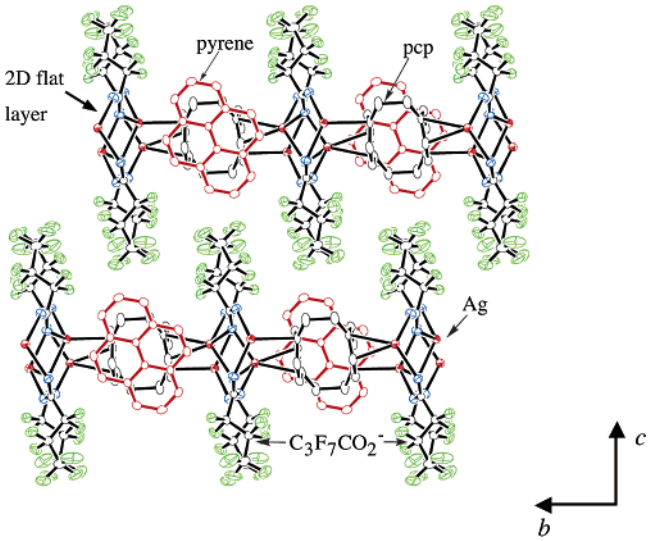

Figure 2. View along the *a*-axis of **1**, showing the moieties of anions perpendicular to the 2D flat layers and the offset packing of adjacent layers.

of three O atoms from three different $C_3F_7CO_2^-$ anions and one C atom of pcp, respectively, as shown in Figure 3a. The Ag−C and Ag−O bond lengths are listed in Table 2. Ligand pcp exhibits unprecedented μ-tetra-η^1 coordination mode.[15] The separation of adjacent sheets is about 11.8 Å. Complex **3** is isostructural with complex **2**, which is confirmed by the X-ray crystallographic determination (Table 1, Figure S1) and X-ray powder diffraction patterns (Figure S2).

$[Ag_4(pcp)(C_3F_7CO_2)_4]\cdot$2benzene (4). The molecular structure and atom numbering scheme of **4** are given in Figure 4a. Both Ag(1) and Ag(2) are four-coordinate, including one C═C moiety of pcp and three O atoms of three different carboxylate groups, respectively. Each pcp exhibits μ-tetra-η^2 coordination mode. The guest benzenes are intercalated between the zigzag layers via edge-to-face $\pi-\pi$ interactions between host pcp and guest benzene with H···C distance of 2.80 Å as shown in Figure 5. Distance between benzene molecules is 4.0 Å, which is beyond the distance for significant $\pi-\pi$ interactions. There also exist cavities of 7.8 Å × 7.0 Å in the intralayer. However, two C_3F_7 groups are on the upper and lower of each cavity, respectively, which do not allow guest benzene molecules to enter the cavities (Figure 4b). The separation of interlayers is 14.9 Å, which is much larger than those of **1**−**3** and consistent with the longer *c* of **4**, which corresponds to the separation between the adjacent layers.

3.2. Guest Exchange. TG analysis revealed that **1** cannot liberate pyrene mainly because of the higher boiling point of pyrene, and the structural decomposition occurs at about 195 °C. However, **1** can exchange pyrene for benzene by

(13) (a) Ning, G. L.; Wu, L. P.; Sugimoto, K.; Munakata, M.; Kuroda-Sowa, T.; Maekawa, M. *J. Chem. Soc., Dalton Trans*. **1999**, 2529. (b) Munakata, M.; Wu, L. P.; Kuroda-Sowa, T.; Maekawa, M.; Suenaga, Y.; Ning, G. L.; Kojima, T. *J. Am. Chem. Soc*. **1998**, *120*, 8610. (c) Fukui, K.; Imamura, A.; Yonezawa, T.; Nagata, C. *Bull. Chem. Soc. Jpn.* **1961**, *34*, 1076. (d) Griffith, E. A. H.; Amma, E. L. *J. Am. Chem. Soc*. **1974**, *96*, 743.

(14) (a) Nishio, M.; Hirota, M.; Umezawa, Y. *The CH/pi Interaction.* Wiley-VCH: New York, **1998**. (b) Burley, S. K.; Petsko, G. A. *Science* **1985**, *229*, 23.

(15) (a) Munakata, M.; Wu, L. P.; Ning, G. L.; Kuroda-Sowa, T.; Maekawa, M.; Suenaga, Y.; Maeno, N. *J. Am. Chem. Soc*. **1999**, *121*, 4968. (b) Munakata, M.; Liu, S. Q.; Konaka, H.; Kuroda-Sowa, T.; Maekawa, M.; Nakagawa, H.; Yamazaki, Y. *Inorg. Chem*. **2004**, *43*, 633. (c) Maekawa, M.; Hashimoto, N.; Sugimoto, K.; Kuroda-Sowa, T.; Suenaga, Y.; Munakata, M. *Inorg. Chim. Acta*. **2003**, *344*, 143 and references therein. (d) Schmidbour, H.; Bublak, W.; Huber, B.; Reber, G.; Müller, G. *Angew. Chem., Int. Ed. Engl*. **1986**, *25*, 1089. (e) Swann, T.; Hanson, A. V.; Boekelheide, V. *J. Am. Chem. Soc*. **1986**, *108*, 3324. (f) Zander, M. *Z. Naturforsch., A: Phys. Sci.* **1984**, *39*, 1009.

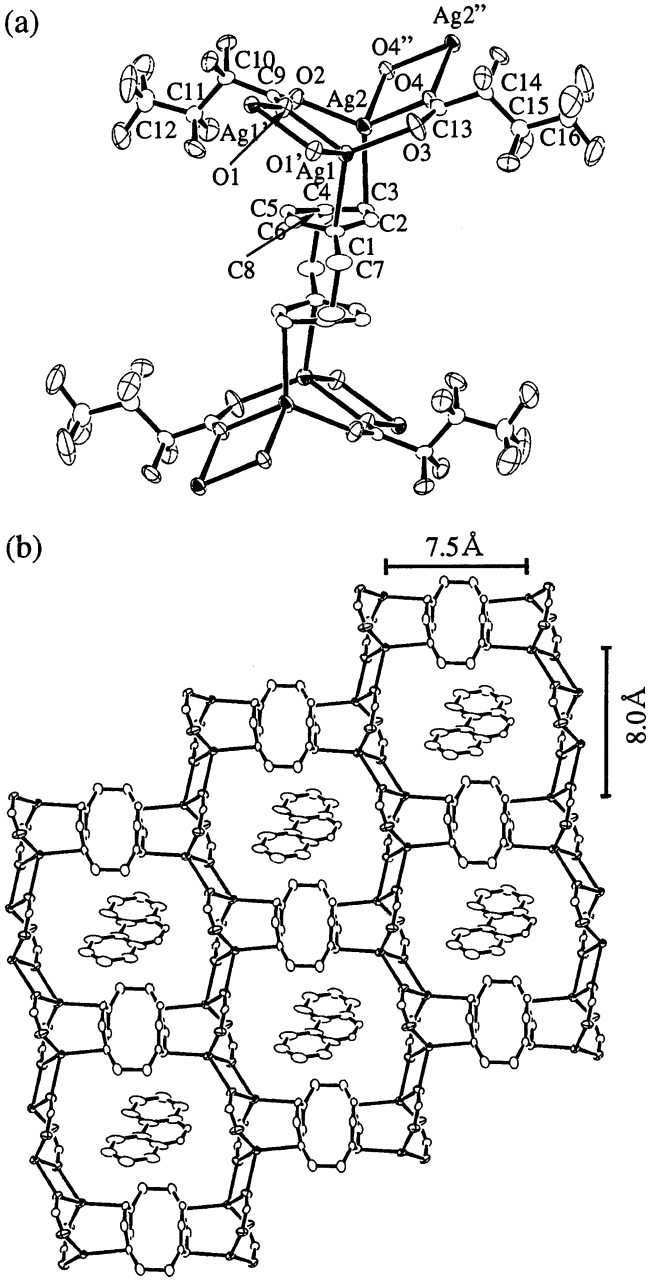

Figure 3. (a) Molecular structure and labeling of **2**. (b) Viewed along the crystallographical *c*-axis, the 2D network of **2** with disordered phenanthrene molecules in cavities. All H atoms and C_3F_7 groups are omitted for clarity.

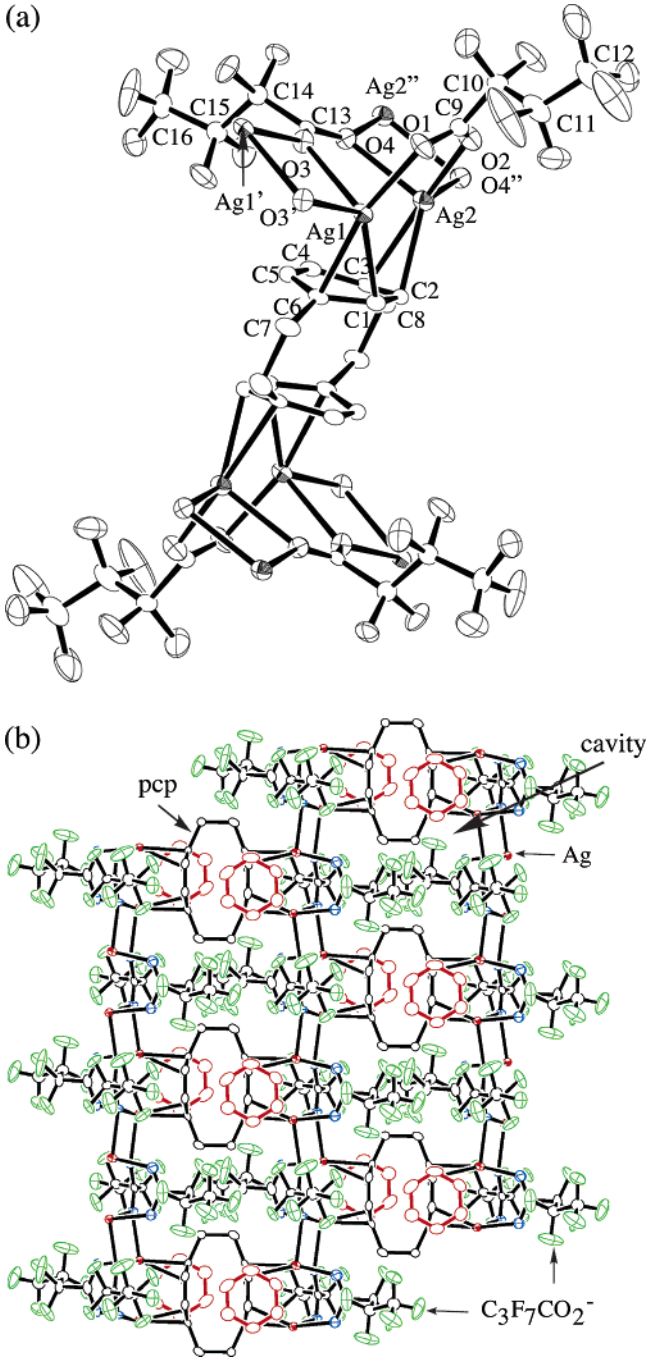

Figure 4. (a) Molecular structure and atom numbering scheme of **4**. (b) View along the *c*-axis of **4**, showing 2D network with benzene molecules up and down the layer. All H atoms are omitted for clarity.

immersing **1** in benzene for 30 min to produce **4a**, which is confirmed by ^{1}H NMR spectra in d_6-acetone and X-ray powder diffraction (XRPD) pattern. ^{1}H NMR resonances of pyrene were observed in **1** but were not observed in **4a**, while those of benzene appeared in **4a** (Figures S3a and S4b). In light of ^{1}H NMR spectra of **4a**, two molecules of benzene per formula unit were included, which is consistent with that of **4**. Figure 6a−c shows the simulated powder pattern obtained from the single-crystal data of **4**, the observed XRPD pattern of as-synthesized sample **4**, and that of **4a**, respectively. The good agreement between the peaks in the three diagrams demonstrates that the structure of **4a** is identical with that of **4**, and complex **1** changes into intercalation compound **4** by guest exchange. The initial framework of **1** undergoes a change to become that of **4** as shown in Figure 7; for instance, a peak (001) at 7.44° for **1** moves to 5.94° for **4**, exhibiting an apparent increase in the layer distance, whereas peaks at 9.20° (100) and 9.68° ($10\bar{1}$) for **1** shift to 10.04° and 10.64° for **4**, respectively, indicating shrinking along planes (100) and ($10\bar{1}$). Notably, **4a** can again exchange benzene for pyrene to afford **1a** (= **1**) by immersing **4a** in pyrene/tetradecane for 6 days at room temperature,[16] and the original framework of **1** was completely recovered as shown in Figure 8a−c. The XRPD pattern of **1a** obtained by guest exchange is virtually identical

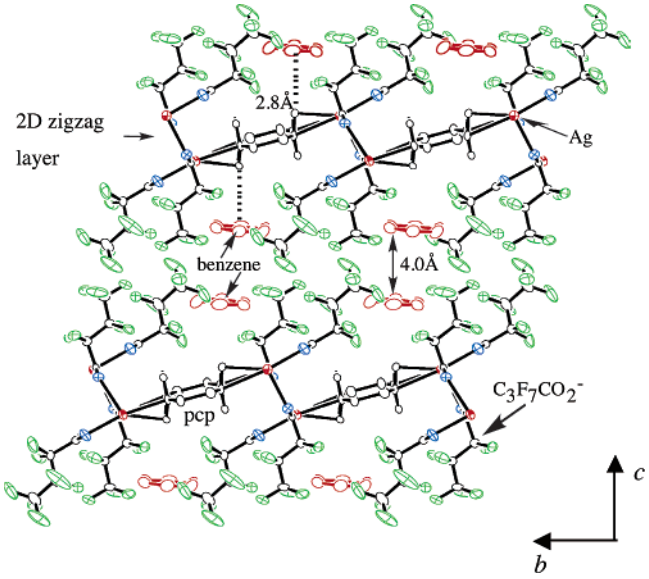

Figure 5. View along the *a*-axis of **4**, showing the guest molecules of benzene intercalated between the zigzag layers.

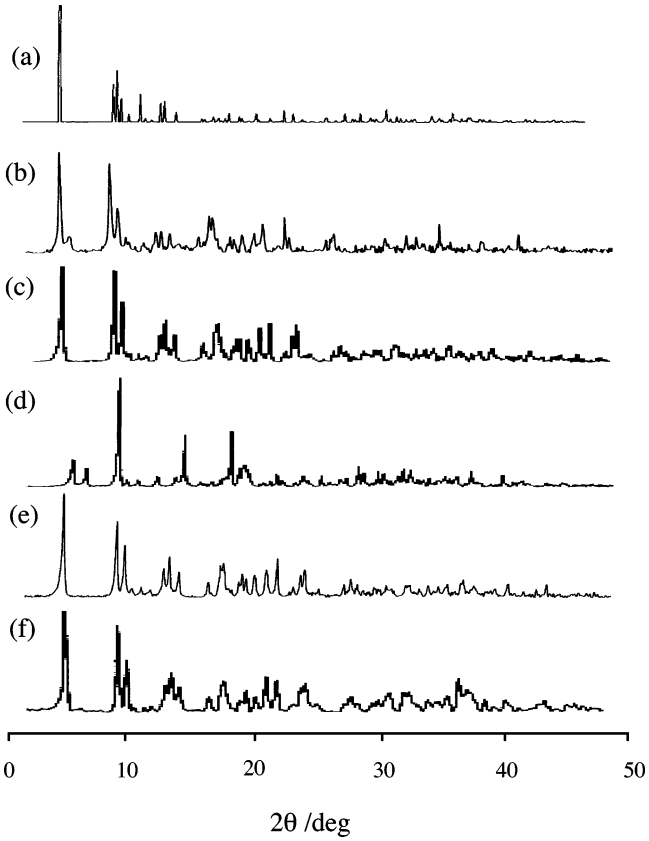

Figure 6. XRPD patterns of **4**, **4a**, and derivatives of **4a**. (a) Simulated XRPD pattern upon a single crystal of **4**. (b) Observed XRPD pattern of as-synthesized sample **4**. (c) **4a** obtained by immersing **1** in benzene for 30 min. (d) **4b** obtained by placing **4a** at 150 °C for 15 min. (e) **4c** obtained by immersing **4b** in benzene for 1 h. (f) **4d** obtained by exposing **4b** to benzene vapor for 1 day.

with that of as-synthesized solid **1**, not only with respect to the positions of the peaks but also the sharpness of the lines, which illustrates the isostructure of **1** and **1a**. In light of ^{1}H NMR of **1a** (Figure S3b), one molecule of pyrene was included. These findings show reversible structural

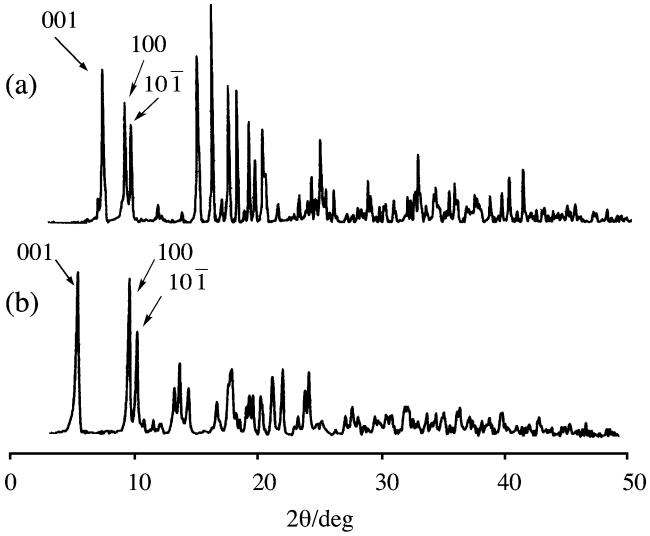

Figure 7. Comparison of XRPD patterns between as-synthesized sample **1** (a) and **4a** obtained by guest exchange from pyrene to benzene (b).

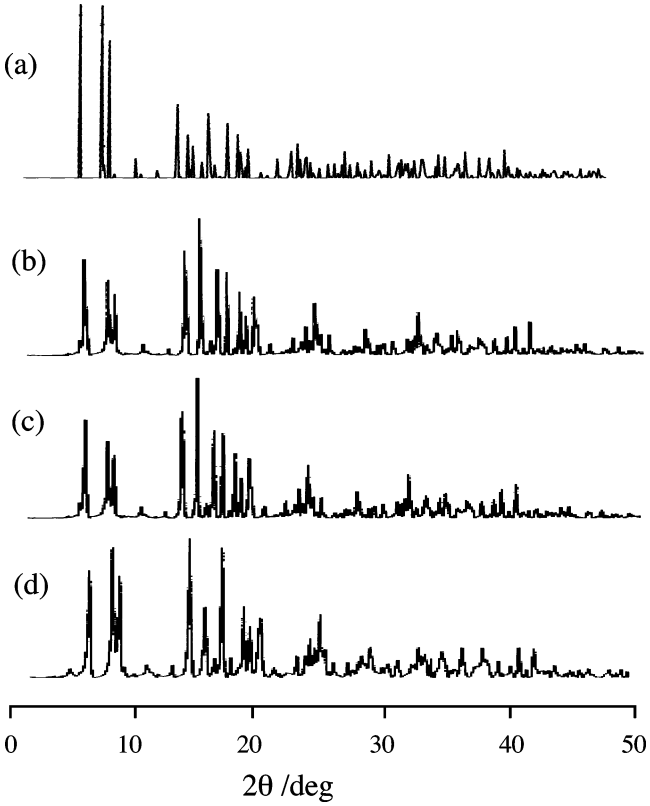

Figure 8. XRPD patterns of **1** and its derivatives. (a) Simulated XRPD pattern upon single-crystal data of **1**. (b) Observed XRPD pattern of as-synthesized sample **1**. (c) **1a** obtained through guest exchange by immersing **4a** in pyrene/tetradecane for 6 days. (d) **1b** obtained through adsorption by immersing **4b** in pyrene/tetradecane for 4 days.

transformation between network **1** and intercalation compound **4**.

(16) Complex **4a** or **4b** cannot dissolve in pyrene/tetradecane, phen/tetradecane, and fluorene/tetradecane. Insolubility was checked by ^{1}H NMR spectra measured with acetone-d_6 solution as illustrated by the following: after **4a** or **4b** was immersed in pyrene/tetradecane, phen/tetradecane, or fluorene/tetradecane, the resulting solution was used to do ^{1}H NMR measurements every 12 h during the whole exchange process, which showed no peak corresponding to [2.2]paracyclophane from the framework of **4a** or **4b**.

Scheme 1

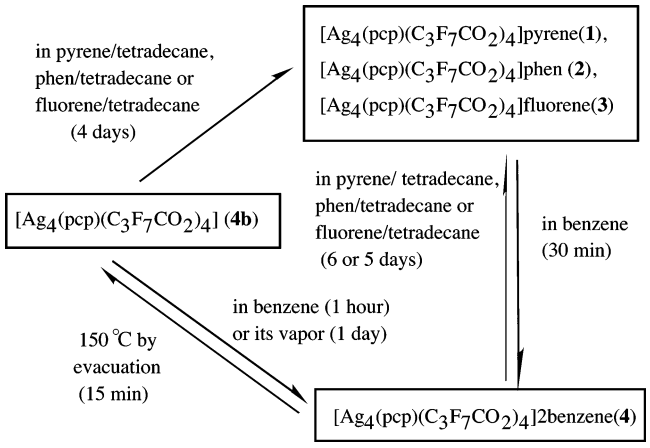

Complexes **2** and **3** show the same exchange behavior as complex **1** (see Supporting Information, Figures S5, S6, S7, and S8).

It is noteworthy that the guest exchange processes in this study occur where the guest is not only solvent (benzene) but also solute (pyrene, phen, or fluorene). As we know, the guest exchange processes are very common in a solvated system, even for coordination complexes.[8] To our knowledge, this is the first report on the guest exchange between the solvated guest molecules and the solute molecules for metal−organic inclusion complexes.

3.3. Reversible Incorporation of Benzene in Complex 4. 4a (= **4**) shows reversible incorporation of benzene. TG analysis measured by evacuating **4a** at 150 °C for 15 min showed the release of benzene with the weight loss of 9.07% (Calcd 9.48%) to give benzene-eliminated complex **4b**. The complete elimination of benzene is also supported by ^{1}H NMR of **4b** (Figure S4c), in which ^{1}H NMR resonances of benzene were not observed. The resulting complex **4b** was then subjected to XRPD analysis against that of **4a** (Figure 6c and d). The XRPD pattern of **4b** has sharp diffraction peaks, indicating that complex **4a** still appears crystalline even without guest molecules. However, the framework of **4a** undergoes slight changes to become that of **4b**. In practice, the recovery of the original structure of **4a** can be accomplished by immersing **4b** in benzene for 1 h (**4c**) as well as by exposing **4b** to benzene vapor for 1 day (**4d**), which is supported by ^{1}H NMR spectra (Figure S4d and e) and XRPD patterns (Figure 6e and f). The peaks in Figure 6c and e and f match very well, illustrating the reversible incorporation of benzene in **4a** (= **4**).

Importantly, **4b** can incorporate pyrene as a guest molecule in the process of immersing **4b** in pyrene/tetradecane for 4 days[16] to produce **1b**, whose structure is the same as that of **1**. This can be confirmed by their XRPD patterns that match very well (Figure 8b and d) as well as ^{1}H NMR spectra (Figure S3c) that show one molecule of pyrene was incorporated in **1b**. The same phenomenon was observed when immersing **4b** in phen/tetradecane or fluorene/tetradecane for 4 days. That is, **4b** can incorporate phen and fluorene as guest molecules to give **2** and **3**, respectively (see Supporting Information, Figures S5d, S6e, S7d, and S8e). The above findings indicate that both the incorporation of guest benzenes in **4a** (= **4**) and the structural transformation between complexes **1**−**3** and intercalation compound **4** caused by guest exchange or guest adsorption can take place reversibly.

4. Conclusion

Herein, we have presented four silver(I) complexes constructed by metal−π bonds and their attracting properties of the reversible structural transformation caused by guest exchange or guest adsorption (Scheme 1). Complexes **1**−**3** are novel 2D networks with cavities that are occupied by guest molecules. They can exchange pyrene, phen, and fluorene for benzene to give intercalation compound **4**, respectively, and vice versa. It is very unusual and interesting that the guest exchange processes occur between the solvated guest molecules and the solute molecules. Meanwhile, complex **4** can reversibly incorporate benzene, and the original framework of **4** is recovered when immersing **4b** in benzene for 1 h as well as exposing **4b** to benzene vapor for 1 day. Furthermore, **4b** can adsorb pyrene, phen, and fluorene as guest molecules to give complexes **1b** (= **1**), **2**, and **3**, respectively. The present complexes **1**−**4** and their intriguing properties make it possible to construct novel functional materials by incorporating photochromic, magnetic, and fluorescent guest molecules. Our investigations in this area are in progress.

Acknowledgment. This work is partially supported by a grants-in-aid for science research (Nos. 14340211 and 16350037) from the Ministry of Education, Science, Sports, and Culture in Japan.

Supporting Information Available: Molecular structure and labeling of **3**, comparison of XRPD patterns of as-synthesized samples **1**, **2**, and **3** showing isostructure, ^{1}H NMR spectra of complexes **1**, **2**, **3**, and **4** and their derivatives, XRPD patterns of as-synthesized samples **2** and **3**; crystallographic data for complexes **1**−**4** in CIF format. This material is available free of charge via the Internet at http://pubs.acs.org.

IC0400742